

Real Option Pricing using Quantum Computers

Alberto Manzano^a,

Gonzalo Ferro Costas^b,

Álvaro Leitao^a,

Carlos Vázquez^a

and Andrés Gómez^b.

*^aDepartment of Mathematics and CITIC,
Universidade da Coruña, A Coruña, Spain*

*^bCentro de Supercomputación de Galicia (CESGA),
Santiago de Compostela, Spain*

Abstract

We present a novel methodology to price derivative contracts using quantum computers by means of Quantum Accelerated Monte Carlo. Our contribution is an algorithm that permits pricing derivative contracts with negative payoffs. Note that the presence of negative payoffs can give rise to negative prices. This behaviour cannot be captured by existing quantum algorithms. Although the procedure we describe is different from the standard one, the main building blocks are the same. Thus, all the extensive research that has been performed is still applicable. Moreover, we experimentally compare the performance of the proposed methodology against other proposals employing a quantum emulator and show that we retain the speedups.

Contents

1	Introduction	3
2	Preliminaries	3
2.1	Classical Monte Carlo for derivatives pricing	4
2.1.1	Simulation of sample paths of the underlying price	4
2.1.2	Integration by Monte Carlo	5
2.2	Quantum Accelerated Monte Carlo for derivatives pricing	5
2.2.1	Quantum simulation	6
2.2.2	Amplitude estimation	8
2.2.3	QAMC simplifications and practical implementation	9
3	Main contributions	11
3.1	Direct encoding	11
3.2	Amplitude estimation	13
4	Conclusions	14
5	Declarations	15
5.1	Ethical Approval and Consent to participate	15
5.2	Consent for publication	15
5.3	Availability of supporting data	15
5.4	Competing interests	15
5.5	Funding	15
5.6	Authors' contributions	15
5.7	Acknowledgements	15
A	Configuration of experiments	17
A.1	Price Estimation problems	17
A.2	Square root encoding Evaluation.	18
A.3	Direct encoding evaluation	19

1 Introduction

Over the last few years there has been an increasing interest in the application of quantum computing to quantitative finance. One of the reasons for such boost of popularity is because many algorithms used by financial institutions demand a high computing capacity and quantum computing promises relevant speedups in some significant relevant cases. Among the different financial applications that could benefit from the use of quantum computing, in this work we focus on the task of pricing financial derivatives.

As it is well known in the literature (see for instance [Góm+22; Gla04]), the pricing of financial derivatives can be formulated in terms of the computation of the expectation of the derivatives payoff with respect to a given probability measure. This computation can be very consuming in terms of computational resources and is typically performed by means of Monte Carlo (MC) methods. In the context of general MC methods, the quantum computing community has proposed a quantum version which can obtain quadratic speedups for very general settings as indicated in [Mon15]. We will refer to such techniques as Quantum Accelerated Monte Carlo (QAMC). They have been successfully applied to the problem of pricing financial derivatives (see [RGB18; Sta+20]).

However, to the best of our knowledge, in the setups treated in the literature, it is implicitly assumed that the price and the payoff of the derivative are strictly positive. Although this is usual for a large number of financial derivatives (as is the case with most of the options traded in the markets) this is not always true. In this manuscript, we propose new quantum algorithms for solving these issues, while retaining the same speedup of previous proposals.

There are three main contributions in this work. First, we propose a new encoding technique called direct encoding. Second, we employ the Real Quantum Amplitude Estimation (RQAE) algorithm [MML23] which is sensitive to the sign of the quantity of interest. The combination of the aforementioned components allows pricing derivative contracts with negative payoffs. Note that negative payoffs potentially entails negative prices. Finally, we perform an experimental assessment of the different encoding and amplitude estimation algorithms for some relevant financial products.

The manuscript is organised as follows. Section 2 is devoted to revise the preliminaries which are at the basis of the article. More precisely, Sections 2.1 and 2.2 contain a brief summary of the classical and quantum techniques to tackle the derivative pricing problem. Section 3 is devoted to the main contributions of the present article. The first part, in Section 3.1, presents the direct encoding for negative payoffs along with its empirical evaluation. The second part, in Section 3.2, leverages the RQAE algorithm for the pricing of derivative contracts with negative prices and again performs an empirical assessment. In Section 4 we summarize the main conclusions. Appendix A contains the configuration of the numerical experiments.

2 Preliminaries

A financial derivative is a financial contract whose price depends on the future prices of another asset or set of assets (usually referred as underlying assets). The derivative price is determined by the future cashflows that will be received which depend on the underlying asset prices. In the present work, we focus on the case where a future payoff is expected at a certain future date (maturity date) and we assume just one underlying asset. Inside this framework, we can find one of the most classical derivatives: European vanilla options. In these derivatives, the owner has the right (but not the obligation) to trade the underlying asset at a given price (strike price) at maturity. Call options provide the right to buy the underlying, while put options provide the right to sell. Therefore, the payoff at maturity is a nonlinear positive function of the asset price. If the derivatives contract involves the obligation to buy or sell (instead of the right), then the payoff function is linear and maybe negative or positive.

Derivatives pricing consists of obtaining the price of the derivative at any previous date to maturity date. For this purpose, the uncertain future dynamics of the price of the underlying asset must be taken into account, which is usually modelled in terms of stochastic differential equations. More precisely, if we denote by S_t the price of the underlying asset at time t , a general Itô process that satisfies the following Stochastic Differential Equation (SDE) can be considered:

$$dS_t = \alpha(t, S_t) dt + \beta(t, S_t) dW_t, \quad (1)$$

where α and β are real functions to be specified for the particular model, while W_t denotes a Brownian motion, so that W_t follows a $\mathcal{N}(0, t)$ distribution (and its increment dW_t follows a $\mathcal{N}(0, dt)$).

Another ingredient in the derivatives pricing is the already mentioned payoff value. We denote by V_t the price of the derivative at time $t \in [0, T]$, where T is the maturity date. Moreover, we assume the existence of a function V , such that $V_t = V(t, S_t)$, i.e., the value of the derivative depends on time and on the underlying asset price through a function V . As stated before, in this work we will focus on derivatives whose payoff only depends on the value of the asset at maturity, $V_T = F(S_T)$, where F represents the payoff function. Next, if we denote the strike price by K , some examples of payoff are:

- European call option: $F(x) = \max(x - K, 0)$.
- European put option: $F(x) = \max(K - x, 0)$.
- Linear payoff: $F(x) = x - K$.

Note that, while the two first payoffs are nonnegative for any value of S_T , the third one can be either positive or negative, depending on S_T .

By using mathematical finance tools, mainly martingale properties and Itô's lemma, the following expression for price of the derivative at time t can be obtained (see for example [Hul97]):

$$V_t = V(t, S_t) = e^{-\int_t^T r_u du} \mathbb{E}_Q[F(S_T)|\mathcal{F}_t], \quad (2)$$

where \mathbb{E}_Q denotes the expectation under the risk neutral measure Q , r_u is the risk-free interest rate at time u , F defines the payoff of the derivative and \mathcal{F}_t denotes the filtration containing the information until time t . In this way, expression (2) indicates that the value of the derivative is the discounted price of the expected value of the payoff, conditioned to the current information of the market.

In view of the pricing expression (2), the valuation of these financial derivatives mainly requires the computation of the involved expectation. Next, we briefly introduce one of the most popular techniques for computing such expectation, namely the Monte Carlo method. We revise the Classical Monte Carlo (CMC) in Section 2.1 and the Quantum Accelerated Monte Carlo (QAMC) in Section 2.2.

2.1 Classical Monte Carlo for derivatives pricing

The CMC method for derivatives pricing in finance is composed of two steps:

1. Simulation of sample paths of the underlying asset by means of the numerical solution of the stochastic differential equation (1).
2. Use of Monte Carlo integration to compute the expectation that appears in expression (2).

2.1.1 Simulation of sample paths of the underlying price

For the simulation of the sample paths, there exist several numerical methods for solving the associated SDE. To illustrate the whole procedure we will use hereon the Euler-Maruyama method as an example. The application of the Euler-Maruyama scheme to the general SDE (1) leads to the expression [AP05]:

$$S_{t+\Delta t} = S_t + \alpha(t, S_t)\Delta t + \beta(t, S_t)\sqrt{\Delta t}Z, \quad (3)$$

where Z is the standard normal random variable, i.e. with mean equal to 0 and variance equal to 1, and Δt is the time step that is considered in the numerical method. In this case, $\Delta t = (T - t)/M$, M

being the number of time steps, T the maturity date and t the initial time. By using Equation (3), it is straightforward to produce samples of S_T , starting from a value of S_t at time t . More precisely, we proceed as follows:

- Start with an initial point S_t .
- Draw a sample of the standard normal random variable Z .
- Compute $S_{t+\Delta t}$ from the random sample generated in the previous step.
- Repeat the previous process, starting from the previously calculated value, until a sample of S_T is obtained.

2.1.2 Integration by Monte Carlo

The procedure described in Section 2.1.1 generates samples S_T^i of the random variable S_T , which can be then used to estimate the expectation that appears in expression (2) as follows:

$$\mathbb{E}[F(S_T)|\mathcal{F}_t] = \frac{1}{N} \sum_{i=0}^{N-1} F(S_T^i) + \epsilon_{CMC} + \epsilon_{EM}. \quad (4)$$

In expression (4), N is the number of samples (paths) S_T^i generated by numerically solving the SDE, F is the payoff function of the target derivatives contract, ϵ_{CMC} is the error due to the Monte Carlo approximation of the expectation and ϵ_{EM} is the error due to the Euler-Maruyama scheme. The statistical error ϵ_{CMC} scales as [Gla04]:

$$\epsilon_{CMC} \sim \frac{1}{\sqrt{N}}. \quad (5)$$

The order of the error due to the Euler-Maruyama scheme is [KP13]:

$$\epsilon_{EM} \sim \Delta t \sim \frac{1}{M}. \quad (6)$$

Taking the definition of the total cost of the algorithm, C_{CMC} as the number of calls to the Euler-Maruyama formula defined in Equation (3), it is straightforward to derive that the total cost is approximately $C_{CMC} \approx MN$. Hence, the overall error of the algorithm ϵ scales with the cost as:

$$\epsilon \sim \frac{1}{\sqrt{C_{CMC}}}. \quad (7)$$

2.2 Quantum Accelerated Monte Carlo for derivatives pricing

The QAMC for pricing has three main ingredients:

- A quantum circuit which samples paths with the same probability as the classical circuit.
- An operator which encodes the payoff of the specific derivative contract into the quantum state.
- An amplitude estimation routine, which allows to retrieve the quantity of interest from the amplitude of a quantum state (and produces the actual speedup).

In Section 2.2.1 we briefly discuss the first issue, while we reserve Section 2.2.2 for the second and third issues.

2.2.1 Quantum simulation

The QAMC algorithm begins by creating a state in superposition where the probabilities of each path match those of the classical process discretized by using some numerical scheme such as the Euler-Maruyama formula. In order to build the algorithm, $M + 1$ different registers are needed, one for each time step. The first M registers are composed of two registers of n_{qb} qubits each (see Figure 1a):

$$[|0\rangle|0\rangle]_0 \otimes [|0\rangle|0\rangle]_1 \otimes \dots \otimes |0\rangle_M, \quad (8)$$

where $[|0\rangle|0\rangle]_m = [|0\rangle^{\otimes n_{qb}} |0\rangle^{\otimes n_{qb}}]_m$, $m = 0, \dots, M$ and $|0\rangle_M = |0\rangle^{\otimes n_{qb}}$.

Each of the individual registers $|0\rangle^{\otimes n_{qb}}$ will be used to represent a decimal number. For simplicity, it can be understood as a single precision register. In order to generate a state in superposition which matches the probabilities of each path defined by the Equation (3), we need a standard normal sample generator. In the QAMC algorithm, this generator is represented by the unitary operator U_Z which performs the following transformation:

$$U_Z |0\rangle|0\rangle = \sum_{j=0}^{J-1} \sqrt{p_Z(x_j)} |0\rangle|x_j\rangle = |0\rangle|x\rangle, \quad (9)$$

where x is a set of J numbers that can be represented by the n_{qb} qubits from the individual registers and $p_Z(x)$ is a discretized version of the standard normal probability distribution defined in the set of points $x = \{x_0, x_1, \dots, x_{J-1}\}$. Note that, in general, J does not need to be equal to $2^{n_{qb}}$. The efficiency of the transformation (9) is crucial for the overall efficiency of the algorithm. In the best case, this efficiency can be achieved using $O(\log_2(J))$ gates (see [GR02]). In the worst case, it can be achieved in $O(J \log_2(J))$ combining the results in [GR02] and [SBM06].

The first step requires applying the operator U_Z to one of the members of all pairs $[|0\rangle|0\rangle]_i$, thus obtaining the state:

$$[U_Z |0\rangle|0\rangle]_0 \otimes [U_Z |0\rangle|0\rangle]_1 \otimes \dots \otimes |0\rangle_M = \left[\sum_{j=0}^{J-1} \sqrt{p_Z(x_j)} |0\rangle|x_j\rangle \right]_0 \otimes \left[\sum_{j=0}^{J-1} \sqrt{p_Z(x_j)} |0\rangle|x_j\rangle \right]_1 \otimes \dots \otimes |0\rangle_M. \quad (10)$$

In this configuration, the amplitudes encode the square root of the probabilities for all the different combinations of x in the different steps. In order to continue, the left register in the pair $[|0\rangle|0\rangle]_0$ has to be initialised to $|S_t\rangle$:

$$[U_{S_t} |0\rangle|y\rangle]_0 = [|S_t\rangle|y\rangle]_0, \quad \forall |y\rangle. \quad (11)$$

Figure 1 depicts schematically this process.

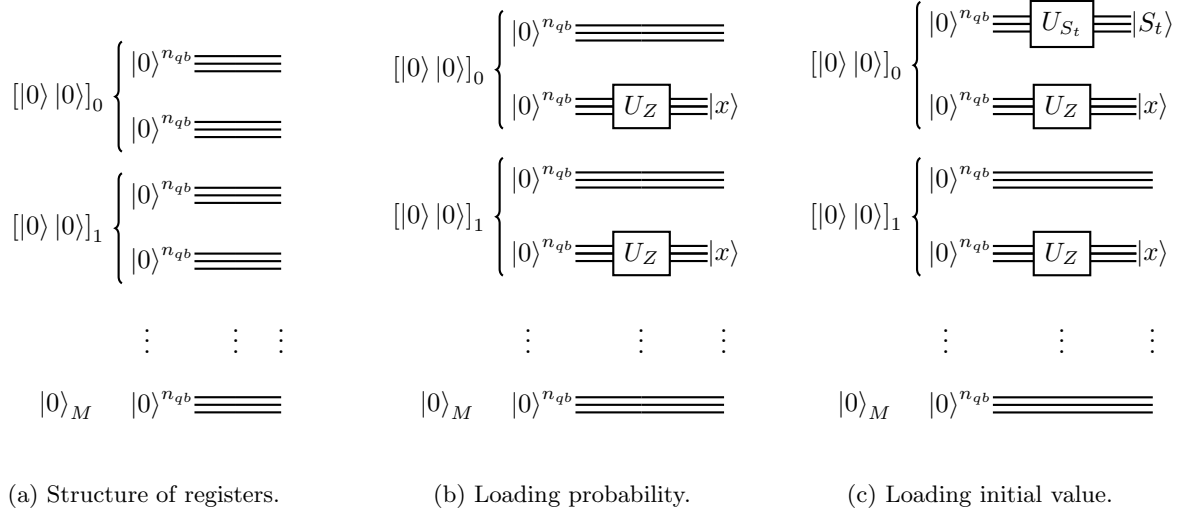


Figure 1: Circuit initialisation.

Once the circuit is correctly initialised, an evolution operator must be applied. This evolution operator acts upon three individual registers as follows:

$$U_{\Delta t} [|S_{t+m\Delta t}\rangle |x\rangle]_m [|0\rangle]_{m+1} \longrightarrow [|S_{t+m\Delta t}\rangle |x\rangle]_m [|S_{t+(m+1)\Delta t}(S_{t+m\Delta t}, x)\rangle]_{m+1}, \quad (12)$$

where the update rule is given, for instance, by Equation (3). After repeatedly applying the operator $U_{\Delta t}$ defined in Equation (12), the final quantum state $|S\rangle$ is:

$$|S\rangle := U_S |0\rangle = \sum_{k=0}^{\mathcal{K}-1} \sqrt{p_S(S_k)} |S_k\rangle, \quad (13)$$

where $\mathcal{K} = J^M$ are the number of possible paths defined by the given (space and time) discretization and $p_S(S_k)$ is the probability of generating the path S_k . Figure 2 depicts schematically this process.

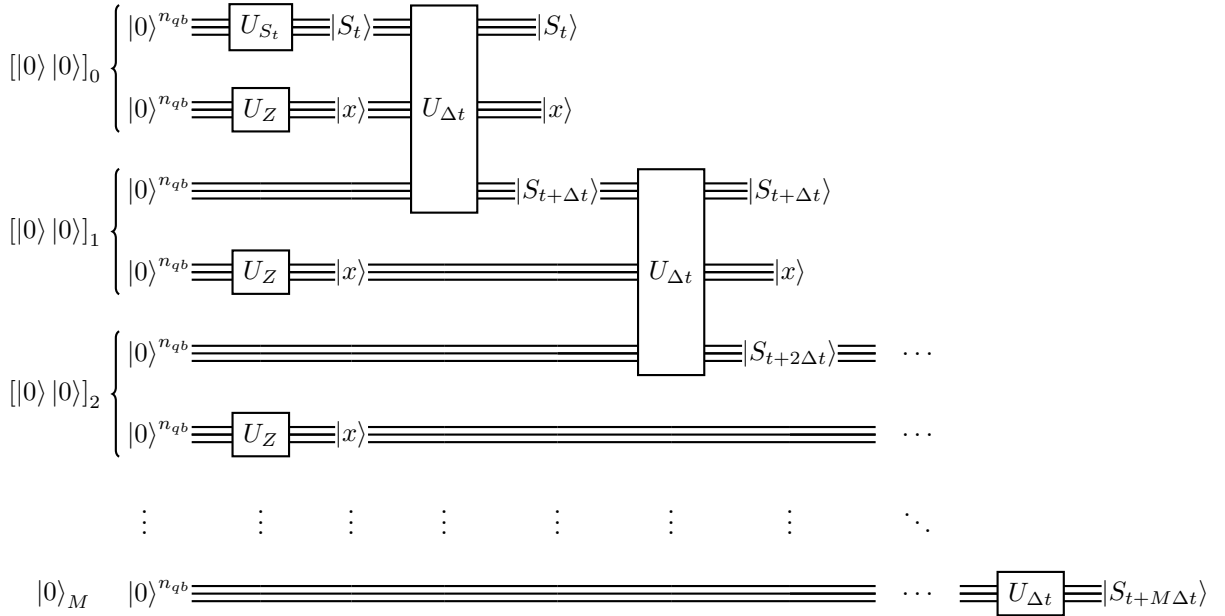


Figure 2: Sketch description of the construction of the oracle defined in Equation (13).

So far, a quantum circuit has been built which samples paths with the same probability as the classical circuit does. Moreover, the computational cost of one execution of the circuit is equivalent to one execution of the classical circuit. In other words, the number of gates needed to sample one path from the classical and the quantum circuit is “the same”, since the classical circuit can always be translated to a quantum one using Toffoli gates (see [NC11]). However, note that classical and quantum gates are not directly comparable.

2.2.2 Amplitude estimation

As discussed in the previous section, up to this point the quantum and the classical circuit have the same complexity. Nevertheless, when the error correction is taken into consideration, the current quantum gates are much slower than the analogous classical ones. Next, the mechanism that produces an speedup is briefly detailed.

Once the state $|S\rangle$ in Equation (13) is generated, the next step is to define the operator $U_{\sqrt{F}}$ such that pushes the square root of the derivatives payoff F into the amplitude. For this reason, we will call this way of encoding *square root encoding*. In order to do that, an additional single qubit register is needed:

$$|\sqrt{F}\rangle = U_{\sqrt{F}}|S\rangle = \frac{1}{\|\sqrt{F(S)}\|_\infty} \sum_{k=0}^{\mathcal{K}-1} \sqrt{p_S(S_k)F(S_k)}|S_k\rangle|0\rangle + \sqrt{p_S(S_k)(1-F(S_k))}|S_k\rangle|1\rangle. \quad (14)$$

For simplicity the term $\|\sqrt{F(S)}\|_\infty$ is considered to be equal to one. In other words, it is assumed to be properly normalised. Moreover, it is tacitly assumed that the operator $U_{\sqrt{F}}$ can be efficiently implemented. Figure 3 depicts schematically the overall process.

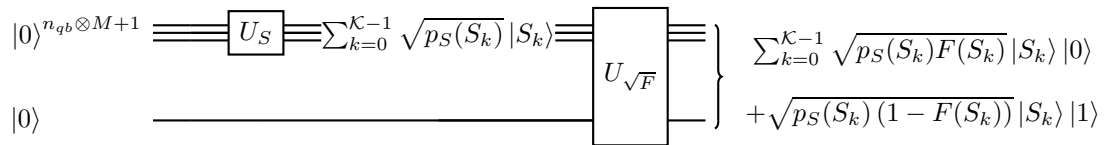


Figure 3: Scheme of the generation of the oracle. The gate U_S corresponds to Equation (13). The gate $U_{\sqrt{F}}$ corresponds to equation (14).

Finally, the expectation of the payoff can be approximated by estimating the probability of obtaining $|0\rangle$ in the last register:

$$\mathbb{E}[F(S_T)|\mathcal{F}_t] = \sum_{k=0}^{\mathcal{K}-1} p_S(S_k)F(S_k) + \epsilon_{\mathcal{K}} + \epsilon_{EM} \approx P_{|0\rangle} + \epsilon_{\mathcal{K}} + \epsilon_{EM} + \epsilon_{QAMC}, \quad (15)$$

where $\sum_{k=0}^{\mathcal{K}-1} p_S(S_k)F(S_k)$ is the discretized expectation, ϵ_{EM} is same Euler-Maruyama error as in Equation (4), $\epsilon_{\mathcal{K}}$ is the discretization error, ϵ_{QAMC} is the sampling error and the expression

$$P_{|0\rangle} = \sum_{k=0}^{\mathcal{K}-1} |p_S(S_k)F(S_k)|$$

is proportional to the exact probability of obtaining the state $|0\rangle$ in the last register.

Using amplitude estimation techniques, the sampling error ϵ_{QAMC} is of order [Bra+02]:

$$\epsilon_{QAMC} \sim \frac{1}{Q}, \quad (16)$$

with Q being the number of calls to the oracle defined by Equation (14). Recall that this oracle is strictly the same as in the classical algorithm described in Section 2.1.1 except for the application of operator $U_{\sqrt{F}}$. Thus, each call to the oracle is equivalent to M executions of the Euler-Maruyama scheme, leading to a total cost of $C_{\text{QAMC}} = MQ$.

Table 1 shows the computational cost, measured in the number of evaluations of the Euler-Maruyama formula, of each of the CMC and the QAMC. It can be easily seen that the QAMC performs quadratically better than the CMC. Moreover, the same scaling applies when we increase the number of dimensions.

	Error
CMC	$O(1/\sqrt{C_{\text{CMC}}})$
QAMC	$O(1/C_{\text{QAMC}})$

Table 1: Comparison of order of the errors for the CMC and the QAMC in one dimension. Both C_{CMC} and C_{QAMC} denote the number of evaluations of the Euler-Maruyama formula.

2.2.3 QAMC simplifications and practical implementation

So far, we have described the general setup of QAMC for pricing. A brief estimation tells us that we would require the order of hundreds or thousands of qubits to build the algorithm with single precision registers and a few time steps. With the current hardware, this is not feasible. Hence, in order to conceptually test this technique, we need to perform several simplifications.

If we assume only European payoffs we can make the first simplification since we do not need to store the whole paths for the underlying. Instead, we will consider that we have just one register which encodes the value of the underlying and we will rewrite it on each step of the Euler-Maruyama scheme. The next simplification would be reducing as much as possible the number of time steps. In the limit, we could perform a single time step. Nevertheless, in numerical schemes such as Euler-Maruyama, a very big time step produces a very big error. For that reason, we restrict ourselves to models where we know how to do exact simulation, thus avoiding the need of doing several steps. This happens when we can obtain the exact solution of the governing SDE. Thus, in this work, we will consider the classical (and well known) model given by the following Black-Scholes SDE under the risk neutral measure [BS73]

$$dS_t = rS_t dt + \sigma S_t dW_t, \quad (17)$$

where r denotes the risk-free rate and σ is the volatility of the underlying asset price. As the expression of the exact solution of SDE (17) is known, starting for a given value S_t , the simulation of the random variable S_T under the risk-neutral measure can be exactly carried out in one step by:

$$S_T = S_t \exp \left(\left(r - \frac{1}{2} \sigma^2 \right) (T - t) + \sigma Z \sqrt{T - t} \right). \quad (18)$$

Under the previously simplified setting, we will only need two-three registers. The first one for storing the initial value of the underlying S_t , the second one would be the register for the standard normal Z and the third one for the final value S_T . Note that, since we only perform one step S_t is not strictly necessary, it can be hardcoded in the operator $U_{\Delta t}$ leaving us with only two registers.

In yet another simplification, we assume that, instead of having a unitary operator U_Z which encodes the standard normal, we have an analogous unitary U_{BS} which encodes the Black-Scholes distribution p_{BS} . With this last simplification, we only need a single register to perform the whole simulation. Note that, regardless all the simplifications, the algorithm is conceptually the same: we have a quantum circuit specified by the oracle $U_S = U_{BS}$ which generates samples for the underlying price with the correct probability distribution.

Throughout the manuscript, we will show different numerical experiments, all of them performed under the simplifications described in this section. For any other content, we will keep ourselves within the general setting from previous sections. For more information on how the experiments are performed, we refer the reader to Appendix A.

To wrap up this section, in Figure 4 we show the results of the QAMC algorithm for different payoffs and amplitude estimation algorithms. If tweaked properly, the best performance is obtained with the Maximum Likelihood Amplitude Estimation (MLAE) [Suz+20]. However, this algorithm requires a fine tuning in the schedule in order to get the best results. For more information on this issue see for example [CB22]. If no fine tuning is performed, the best algorithm is the Iterative Quantum Amplitude Estimation (IQAE)[Gri+21] as it is more stable. The standard (classical) amplitude estimation algorithm (here denoted by CAE) [Bra+02] is stable but, in general, has worse performance.

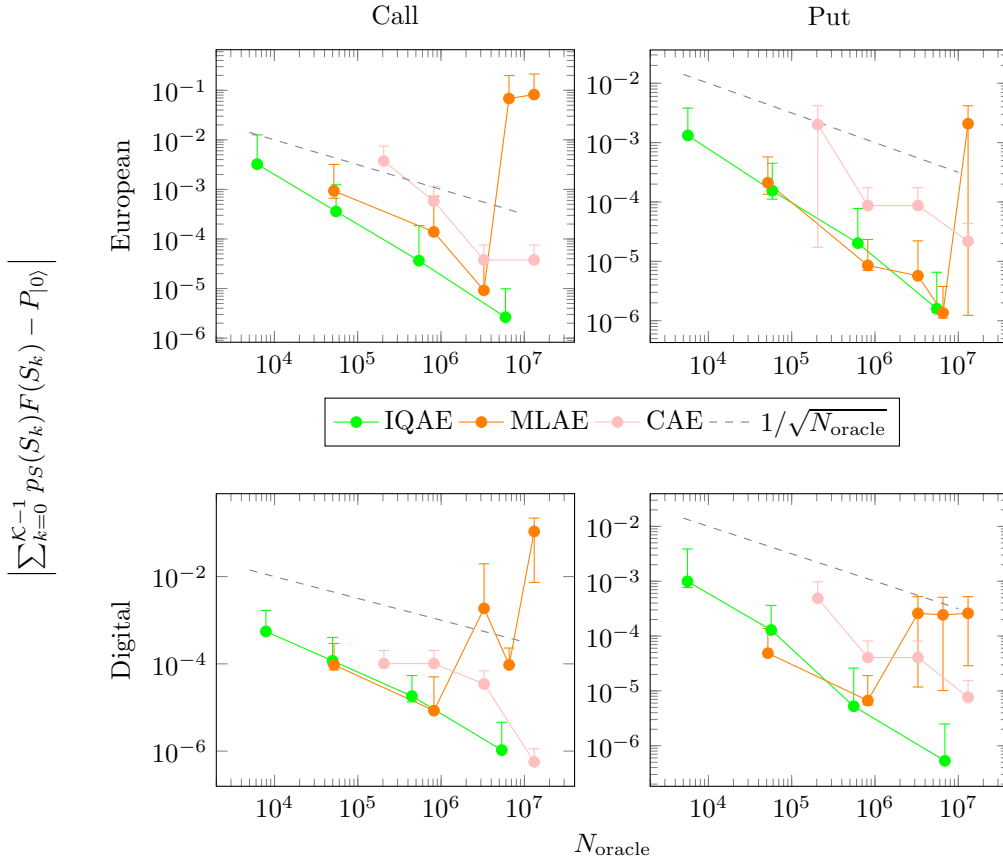


Figure 4: Absolute error between the QAMC algorithm and the discretized expectation for different number of calls to the oracle. Each of the panels corresponds to a different payoff (see A.1 for details) and each line corresponds to a different amplitude estimation algorithm. For a detailed description for the parameters of each simulation, see Table 5. The experiments have been performed using the square root encoding.

3 Main contributions

As it can be seen in Section 2.2.2, by sampling from the quantum circuit an estimation of:

$$\sum_{k=0}^{\mathcal{K}-1} |p_S(S_k)F(S_k)|, \quad (19)$$

can be obtained. Note that the payoff is assumed to be normalised so that $\|\sqrt{F(S)}\|_\infty = 1$.

Nevertheless, it is important to note that, for derivatives whose payoffs can become negative, this method will not yield to correct prices approximations. In order to illustrate this, suppose that there is a payoff of the form:

$$F(S_T) = S_T - K, \quad (20)$$

with T being the maturity of the contract, S_T the price of the underlying at maturity and K the strike price of the contract (see [Góm+22] for details).

In Figure 5, when the square root encoding is used in combination with some of the most well known amplitude estimation algorithms in the literature, it is easily seen that there is no convergence to the real value because of the presence of the absolute value. In Sections 3.1 and 3.2 we develop an strategy to overcome this issue which consists of two parts. On the one hand, a new encoding is proposed. On the other hand, a different amplitude estimation technique is employed.

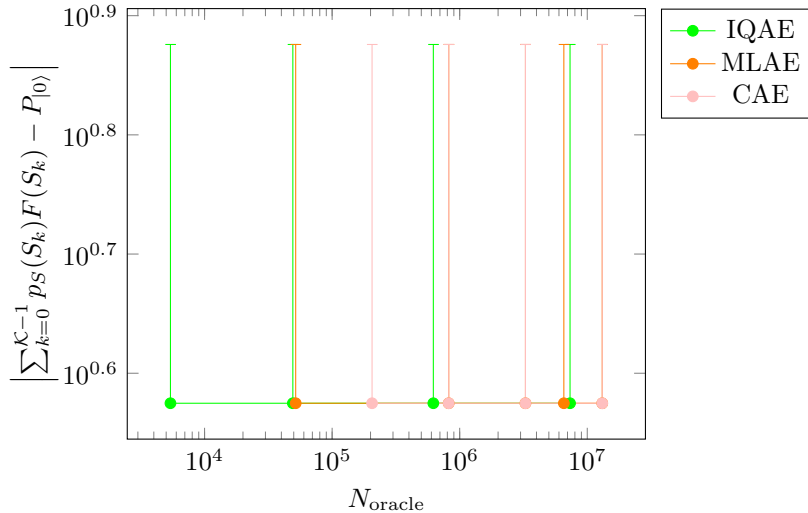


Figure 5: Absolute error between the QAMC algorithm and the discretized expectation of an option with a payoff $(S_T - K)$ with $K = S_t$ for different number of calls to the oracle. Each line corresponds to a different amplitude estimation algorithm. For a detailed description for the parameters of each simulation, see Table 5. The experiments have been performed using the square root encoding.

3.1 Direct encoding

The *direct encoding* algorithm starts from the same initial state $|S\rangle$:

$$|S\rangle = U_S |0\rangle = \sum_{k=0}^{\mathcal{K}-1} \sqrt{p_S(S_k)} |S_k\rangle, \quad (21)$$

where \mathcal{K} is again the number of possible paths defined by the given discretization. The next step is to define the operator U_F such that pushes the payoff without squared roots into the amplitude. In order to do that, an additional single qubit register is needed:

$$|F\rangle = U_F |S\rangle = \frac{1}{\|F(S)\|_\infty} \sum_{k=0}^{\mathcal{K}-1} \sqrt{p_S(S_k)} F(S_k) |S_k\rangle |0\rangle + \sqrt{p_S(S_k)} (1 - F(S_k)) |S_k\rangle |1\rangle. \quad (22)$$

Next, we project the state $|F\rangle$ into $\langle S| \langle 0|$:

$$\langle S| \langle 0|F\rangle = \frac{1}{\|F(S)\|_\infty} \sum_{k=0}^{\mathcal{K}-1} p_S(S_k)F(S_k). \quad (23)$$

In practice, instead of projection, we will apply the adjoint of U_S and then measuring the eigenstate zero (see Figure 6), hence obtaining:

$$\sqrt{\bar{P}_{|0\rangle}} = \left| \langle 0| U_S^\dagger U_F U_S |0\rangle \right| = \frac{1}{\|F(S)\|_\infty} \left| \sum_{k=0}^{\mathcal{K}-1} p_S(S_k)F(S_k) \right|. \quad (24)$$

Do not confuse $P_{|0\rangle}$ from the square root encoding from the $\bar{P}_{|0\rangle}$ in the direct encoding. The former one refers to the probability of measuring zero in the last register when the unitary $U_{\sqrt{F}}U_S$ is applied. The latter one refers to the probability of measuring the eigenstate zero when the unitary $U_S^\dagger U_F U_S$ is applied.

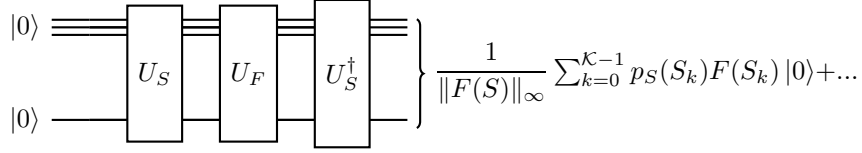


Figure 6: Scheme of the proposed direct encoding.

Hence, an estimation of the discretized expectation is obtained as:

$$\left| \sum_{k=0}^{\mathcal{K}-1} p_S(S_k)F(S_k) \right| = \|F(S)\|_\infty \sqrt{\bar{P}_{|0\rangle}}. \quad (25)$$

Again, in order to achieve a speedup, an amplitude estimation algorithm is needed. As shown in Figure 7, when the direct encoding is used, the result converges to the discretized expectation even when the payoff takes negative values, which is a novelty when compared with other proposed methods in the literature, that cannot deal with these negative values. However, the presence of the outer absolute value in Equation (25) still prevents from a correct estimation when negative expectations arise.

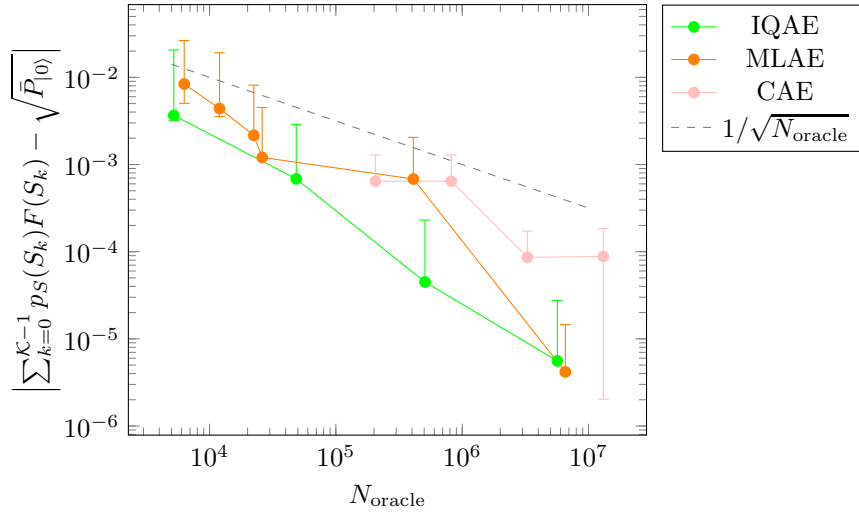


Figure 7: Absolute error between the QAMC algorithm and the discretized expectation of an option with a payoff $(S_T - K)$ with $K = S_t$ for different number of calls to the oracle. Each line corresponds to a different amplitude estimation algorithm. For a detailed description for the parameters of each simulation, see Table 5. The experiments have been performed using the direct encoding.

3.2 Amplitude estimation

At the end of the previous section it was discussed that the discretized expectation can be estimated through the probability of measuring state $|0\rangle$:

$$\sqrt{\bar{P}_{|0\rangle}} \propto \left| \sum_{k=0}^{\mathcal{K}-1} p_S(S_k) F(S_k) \right|.$$

Thus, this partially solves the initial problem. Instead of obtaining the sum of absolute values, something proportional to the absolute value of the sum is returned. Hence, in a situation where the sign of the expectation is of interest, an additional mechanism to overcome this issue is needed. In fact, this is usually the case in financial applications, where the sign is the difference between a profit and a loss.

For this case, we propose to use of the Real Quantum Amplitude Estimation (RQAE) algorithm. Its main property is that it is able to recover the amplitude of the quantum state plus some information on the quantum phase, namely the sign. Another interesting property is that it has a free parameter q , called amplification ratio, which allows the user to control the overall depth of the circuit. Bigger values of q yields shallower circuits but slower convergence, while smaller values of q yields deeper circuits but faster convergence. In Figure 8, an example where the price of the derivative becomes negative is shown. As it can be seen, RQAE is the only algorithm that converges to the exact solution. Further, in Figure 9 we show that the RQAE is also competitive with the most advanced algorithms from the literature in terms of number of calls to the oracle.

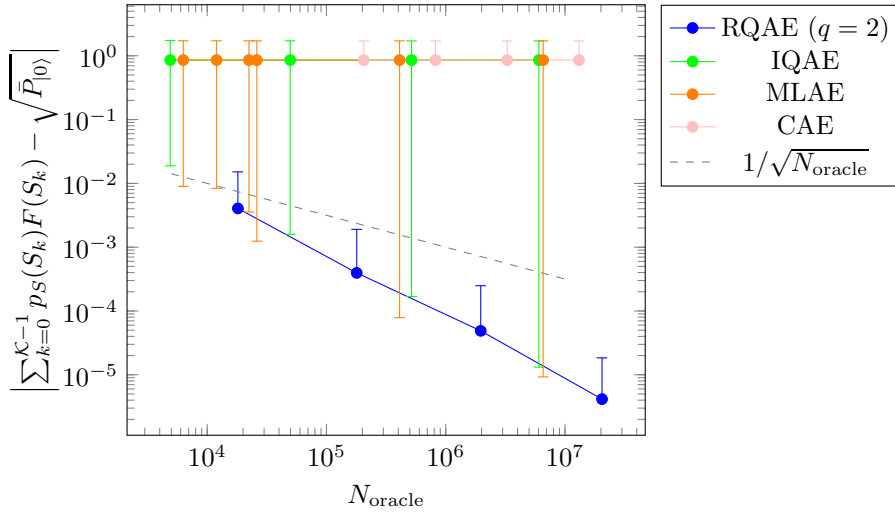


Figure 8: Absolute error between the QAMC algorithm and the discretized expectation of an option with a payoff $(S_T - K)$ with $K = 1.5S_t$ for different number of calls to the oracle. Each line corresponds to a different amplitude estimation algorithm. For a detailed description for the parameters of each simulation, see Table 5. The experiments have been performed using the direct encoding.

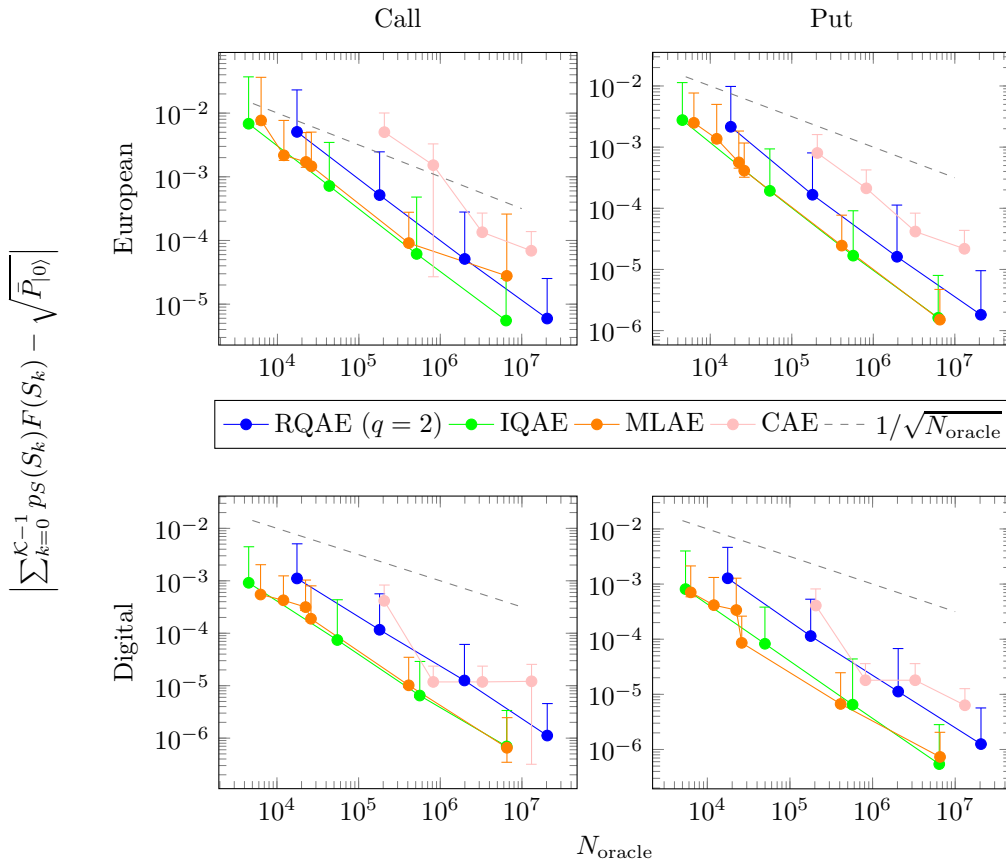


Figure 9: Absolute error between the QAMC algorithm and the discretized expectation for different number of calls to the oracle. Each of the panels corresponds to a different payoff and each line corresponds to a different amplitude estimation algorithm. For a detailed description for the parameters of each simulation, see Table 5.

4 Conclusions

In this work, we have presented two novel proposals for using quantum computers for derivative pricing. On the one hand, we have introduced a new encoding algorithm for the payoff of the derivatives contract, the direct encoding. On the other hand, the use of RQAE as the amplitude estimation routine in the overall pipeline is proposed. The combination of the two allows pricing derivative products with negative payoffs. Moreover, through Sections 3.1 and 3.2, we perform different experiments to validate our methodology. In particular, we have shown that existing alternatives fail for payoffs as simple as $F(x) = x - K$ that involve negative values. Further, the proposed methodology is competitive in terms of “speed” with the best known algorithms.

Although in theory QAMC gets a quadratic speedup over CMC, there are still many issues to solve in practice, specially if we take into consideration the current state-of-the-art hardware constraints. First, the implementation of the oracle U_S as explained in Section 2.2.1 requires an excessively large number of qubits. Second, the depths required by the current Grover-like routines are not feasible under the current decoherence times. Finally, the total number of gates when combining the implementation of oracle U_S with a Grover-like algorithm requires a gate error beyond the capabilities of the current technology.

In future works, we will explore how to face the different previously pointed problems, with special focus in efficiently initializing states that approximately encode a target probability distribution.

5 Declarations

5.1 Ethical Approval and Consent to participate

Not applicable.

5.2 Consent for publication

Not applicable.

5.3 Availability of supporting data

Not applicable.

5.4 Competing interests

The authors declare that they have no competing interests.

5.5 Funding

All authors acknowledge the European Project NExt ApplicationS of Quantum Computing (NEASQC), funded by Horizon 2020 Program inside the call H2020-FETFLAG-2020-01(Grant Agreement 951821).

A. Manzano, Á. Leitao and C. Vázquez wish to acknowledge the support received from the Centro de Investigación de Galicia “CITIC”, funded by Xunta de Galicia and the European Union (European Regional Development Fund- Galicia 2014-2020 Program), by grant ED431G 2019/01.

5.6 Authors’ contributions

5.7 Acknowledgements

The authors would like to thank Vedran Dunjko and Emil Dimitrov for fruitful discussions on some aspects of the present work.

The most part of the computational resources for this work were provided by the Galician Supercomputing Center (CESGA).

References

- [BS73] Fischer Black and Myron Scholes. “The Pricing of Options and Corporate Liabilities”. In: *Journal of Political Economy* 81.3 (1973), pp. 637–654. ISSN: 00223808, 1537534X.
- [Hul97] John C. Hull. *Options, futures, and other derivatives*. 3. ed., internat. ed. Prentice Hall, 1997. URL: <http://gso.gbv.de/DB=2.1/CMD?ACT=SRCHA&SRT=YOP&IKT=1016&TRM=ppn+216058376&source>
- [Bra+02] Gilles Brassard et al. “Quantum amplitude amplification and estimation”. In: *Contemporary Mathematics* 305 (2002), pp. 53–74.
- [GR02] Lov Grover and Terry Rudolph. *Creating superpositions that correspond to efficiently integrable probability distributions*. 2002. DOI: 10.48550/ARXIV.QUANT-PH/0208112. URL: <https://arxiv.org/a>
- [Gla04] Paul Glasserman. *Monte Carlo methods in financial engineering*. New York: Springer, 2004.
- [AP05] Yves Achdou and Olivier Pironneau. *Computational Methods for Option Pricing (Frontiers in Applied Mathematics) (Frontiers in Applied Mathematics 30)*. USA: Society for Industrial and Applied Mathematics, 2005. ISBN: 0898715733.
- [SBM06] V.V. Shende, S.S. Bullock, and I.L. Markov. “Synthesis of quantum-logic circuits”. In: *IEEE Transactions on Computer-Aided Design of Integrated Circuits and Systems* 25.6 (June 2006), pp. 1000–1010. DOI: 10.1109/tcad.2005.855930. URL: <https://doi.org/10.1109%5C%2Ftcad.2005>

- [NC11] Michael A. Nielsen and Isaac L. Chuang. *Quantum Computation and Quantum Information: 10th Anniversary Edition*. Cambridge University Press, 2011. ISBN: 9781107002173.
- [KP13] Peter E Kloeden and Eckhard Platen. *Numerical Solution of Stochastic Differential Equations*. Vol. 23. Springer Science & Business Media, 2013.
- [Mon15] Ashley Montanaro. “Quantum speedup of Monte Carlo methods”. In: *Proceedings of the Royal Society A: Mathematical, Physical and Engineering Sciences* 471.2181 (2015), p. 20150301.
- [RGB18] Patrick Rebstrodt, Brajesh Gupta, and Thomas R. Bromley. “Quantum computational finance: Monte Carlo pricing of financial derivatives”. In: *Physical Review A* 98.2 (Aug. 2018). ISSN: 2469-9934.
- [Sta+20] Nikitas Stamatopoulos et al. “Option pricing using quantum computers”. In: *Quantum* 4 (2020), p. 291.
- [Suz+20] Yohichi Suzuki et al. “Amplitude estimation without phase estimation”. In: *Quantum Information Processing* 19.2 (Jan. 2020). DOI: 10.1007/s11128-019-2565-2. URL: <https://doi.org/10.1007/s11128-019-2565-2>.
- [Gri+21] Dmitry Grinko et al. “Iterative quantum amplitude estimation”. In: *npj Quantum Information* 7.1 (Mar. 2021). DOI: 10.1038/s41534-021-00379-1. URL: <https://doi.org/10.1038/s41534-021-00379-1>.
- [CB22] Adam Callison and Dan E. Browne. *Improved maximum-likelihood quantum amplitude estimation*. 2022. DOI: 10.48550/ARXIV.2209.03321. URL: <https://arxiv.org/abs/2209.03321>.
- [FM22] Gonzalo Ferro and Alberto Manzano. *QQuantLib*. <https://github.com/NEASQC/FinancialApplications>. 2022.
- [Góm+22] Andrés Gómez et al. “A survey on Quantum Computational Finance for derivatives pricing and VaR”. In: *Archives of Computational Methods in Engineering* (Mar. 2022). DOI: 10.1007/s11831-022-09732-9.
- [MML23] Alberto Manzano, Daniele Musso, and Álvaro Leitao. “Real quantum amplitude estimation”. In: *EPJ Quantum Technology* 10.1 (2023), pp. 1–24.

A Configuration of experiments

This appendix gives the detailed configuration of all the experiments performed in this paper (see Figure 4 from Section 2.2.2 and Figures 5, 7, 8 and 9 from Section 3). The proposed experiments consist in pricing different financial derivatives (see Section A.1) using the different methods described throughout the paper. More specifically, in Section A.1 we describe the financial setting, in Section A.2 we present the configuration for the experiments when the standard procedure from Section 2.2.1 is used and, in Section A.3, we specify the configuration of the experiments when the direct encoding from Section 3.1 is employed.

All the experiments were done with the QQuantLib Python library (see [FM22]).

A.1 Price Estimation problems

For all the experiments in the paper we have modelled the underlying S using Black-Scholes dynamics (see Equation (17)) with the parameters from Table 2.

Probability distribution	Initial value (S_t)	Volatility (σ)	Risk free rate (r)
Black-Scholes	1.0	0.5	0.05

Table 2: Financial model and parameters for the underlying used in the evaluation.

We have tested the different methods on different derivative contracts. All of the derivative contracts are summarised in Table 3.

Option	K/S_t	Payoff
European Call Option	0.5	$F(x) = \max(0, x - K)$
European Put Option	1.5	$F(x) = \max(0, K - x)$
Digital Call Option	0.5	$F(x) = 1$ if $x \geq K$, 0 otherwise
Digital Put Option	1.5	$F(x) = 1$ if $x \leq K$, 0 otherwise
Futures	0.5	$F(x) = x - K$
Futures	1.0	$F(x) = x - K$
Futures	1.5	$F(x) = x - K$

Table 3: List of the different derivative contracts with their correspondent payoffs and the strikes, K .

In order to do the pricing, we have applied all the simplifications from Section 2.2.3. Under this simplifications the problem of computing the expectation from Equation (15) is reduced to the problem of computing the integral:

$$\mathbb{E}[F(S_T)|\mathcal{F}_t] = \int_{\mathbb{R}} p_{BS}(x; r, \sigma) F(x) dx,$$

where $p_{BS}(x; r, \sigma)$ is the probability distribution for the Black-Scholes dynamics at maturity T with the free-risk interest rate r and volatility σ :

$$p_{BS}(x; r, \sigma) = \frac{1}{x\sigma\sqrt{2\pi T}} \exp\left(-\frac{(\ln(x) - r)^2}{2\sigma^2 T}\right).$$

In practice, to compute the integral we apply a numerical quadrature. Here we truncate the domain in $[x_0, x_f]$ so that the discretized expectation becomes a Riemann sum of I intervals:

$$\int_{\mathbb{R}} p_{\text{BS}}(x; r, \sigma) F(x) dx \approx \sum_{i=0}^I p_{\text{BS}}(x_i; r, \sigma) F(x_i) \Delta x, \quad (26)$$

with $\Delta x = (x_f - x_0)/I$. The information about the discretization can be found in Table 4.

\mathbf{x}_0	\mathbf{x}_f	$\mathbf{n}_{\text{qbits}}$	Intervals
0.01	5.0	5	32

Table 4: Settings for the discretization in Equation (26).

A.2 Square root encoding Evaluation.

All the information presented in this section refers to the experiments done using the square root (see Section 2.2.1). The amplitude estimation techniques used for the QAMC simulation are the following:

- Classical Quantum Phase Estimation Amplitude Estimation, CAE, see [Bra+02].
- Iterative Quantum Amplitude Estimation, IQAE, see [Gri+21].
- Maximum Likelihood Amplitude Estimation, MLAE, see [Suz+20].

In Table we summarise 5 the parameters for the tested amplitude estimation techniques.

	CAE	IQAE	MLAE
Auxiliar qubits number	10, 12, 14, 16	N/A	N/A
Classical bits number	N/A	N/A	N/A
Epsilon (ϵ)	N/A	$10^{-2}, 10^{-3}, 10^{-4}, 10^{-5}$	NA
Alpha (α)	N/A	0.05	N/A
Number of different schedules	N/A	N/A	5
ns	N/A	N/A	10000
Delta	N/A	N/A	10^{-7}
Shots	100	100	NA
QPU	QLM	FT3	QLM
Repetitions	10	10	10

Table 5: Amplitude estimation algorithms and their corresponding parameters for the square root encoding.

The parameter ‘‘QPU’’ from Table 5 refers to the type of hardware platform where the simulations were done:

- QLM: the simulations were done in the Atos *Quantum Learning Machine* this is a hardware platform for quantum circuit simulator up to 30 qubits: with 96 cores and 1.5 TB of RAM. The *linear-algebra based quantum simulator*, *LinAlg*, from Atos QLM software version 1.5.1 was used.
- FT3: simulations were done in a computation node of the FinisTerra III: Intel Xeon Ice Lake 835Y with 256 GB of RAM and 64 cores¹. The *Python Lineal Algebra* simulator, *PyLinalg*, from Atos myQLM version 1.5.1 was used.

The parameter “Repetitions” in Table 5 is the number of simulations done for each possible combination of the different options (Table 3), amplitude estimation techniques, and parameters (Table 5). As can be seen 10 repetitions were done for each amplitude estimation technique.

The parameters “ns” and “Delta” in Table 5 are configuration parameters of the *brute-force scipy* optimizer used for the MLAE algorithm tests. The former one refers to the number of grid points in which the search domain is divided, while the latter controls to the boundaries of the domain: $(Delta, \frac{\pi}{2} - Delta)$.

A.3 Direct encoding evaluation

All the information presented in this section refers to the experiments done using the direct encoding from Section 3.1. The price estimation problems defined in Tables 2, 3, and 4 were solved using QAMC and the amplitude estimation techniques enumerated in Section A.2. Additionally, we include the RQAE algorithm, see [MML23]. In Table 6 we summarise the parameters for the tested amplitude estimation techniques.

See Section A.2 for the interpretation of “QPU” and “Repetitions”. As we are interested in how the RQAE compares in performance with the standard the facto in the literature (the IQAE), we performed more repetitions of the experiments of these two.

¹The number of cores and the amount of the RAM used depended on the simulations to be executed.

	CAE	IQAE	MLAE	RQAE
Auxiliar qubits number	10, 12, 14, 16	N/A	N/A	N/A
Classical bits number	N/A	N/A	N/A	N/A
Epsilon (ϵ)	N/A	$10^{-2}, 10^{-3}, 10^{-4}, 10^{-5}$	N/A	$10^{-3}, 10^{-4}, 10^{-5}$
Alpha (α)	N/A	0.05	N/A	N/A
Gamma (γ)	N/A	N/A	N/A	0.05
q	N/A	N/A	N/A	1.2, 1.5, 2, 5, 10, 20
Number of different schedules	N/A	N/A	5	N/A
ns	N/A	N/A	10000	N/A
Delta	N/A	N/A	10^{-7}	N/A
Shots	100	100	N/A	N/A
Repetitions	10	100	10	100
QPU	QLM	FT3	QLM	QLM + FT3

Table 6: Amplitude estimation algorithms and their corresponding parameters used for the simulations with the direct encoding.